



# HOKKAIDO UNIVERSITY

Title	Two Case Studies of Heavy Rainfalls from the Stratiform and Convective Precipitation Clouds in the Orofure Mountain Range, Hokkaido, Japan
Author(s)	IWANAMI, Koyuru; KIKUCHI, Katsuhiro; UYEDA, Hiroshi et al.
Citation	Journal of the Faculty of Science, Hokkaido University. Series 7, Geophysics, 10(2), 239-268
Issue Date	1997-02-28
Doc URL	<a href="https://hdl.handle.net/2115/8819">https://hdl.handle.net/2115/8819</a>
Type	departmental bulletin paper
File Information	10(2)_p239-268.pdf



## Two Case Studies of Heavy Rainfalls from the Stratiform and Convective Precipitation Clouds in the Orofure Mountain Range, Hokkaido, Japan

Koyuru Iwanami<sup>1</sup>, Katsuhiko Kikuchi, Hiroshi Uyeda  
and Takashi Taniguchi<sup>2</sup>

*Department of Geophysics, Faculty of Science, Hokkaido University,  
Sapporo 060, Japan*

( Received December 14, 1996 )

### Abstract

Rainfall observations were carried out with mobile weather radar and a special mesoscale network of raingauges, wind vanes and anemometers, and microbarometers from late August to early September in 1985 and 1986 on the southeastern slope of the Orofure mountain range in the southwestern part of Hokkaido, Japan. The rainfalls on September 3 to 4 in 1986 were associated with a depression changed from a typhoon and with northerly surface winds. The stratiform radar echoes extended widely over the observation area and the rainfall amount was distributed over wide areas beyond the southeastern slope of the mountain range. In the first half of this rainfall, the bright band was especially remarkable and the thin distinctive layer appeared below 2.0 km a.s.l. However the surface winds on the region between two ridges running southeastward changed to southerly in the second half, and the radar echoes in the lower layer developed from updrafts produced over the slopes blown by the winds near the ground surface. It is therefore concluded that the topography produced small scale effects on the stratiform precipitation clouds passing over the observation area.

The rainfalls on September 10 to 11 in 1986 occurred under a synoptic situation where the northern part of Japan was covered with a trough and unstable atmosphere. The rainfall amount was concentrated on the southeastern slope of the mountain range, especially in the seaside region, in contrast to the first case. The heavy rainfalls whose intensity reached  $108 \text{ mmhr}^{-1}$  in the seaside region were caused by the deep convective precipitation clouds. It is considered that the forced uplifting of southerly flow from the Pacific Ocean near the ground surface played an important role in the generation and development of the precipitation clouds in the mountainous

---

<sup>1</sup> Present affiliation: Nagaoka Institute of Snow and Ice Studies, National Research Institute for Earth Science and Disaster Prevention, Nagaoka 940, Japan.

<sup>2</sup> Present affiliation: Hokkaido Head Office, Japan Weather Association, Sapporo 064, Japan.

region. In the plain region the precipitation clouds were considered to be maintained by the updrafts caused by convergence over the shear line. Furthermore, it is considered that the updrafts, that were caused by both the convergence over this shear line and the frictional convergence resulting from the roughness discontinuity between land and sea, promoted the development of the band-shaped deep precipitation clouds on the seaside region.

## 1. Introduction

Orographic rainfall has been actively studied to date, particularly in the South Wales hills in the British Isles (Browning et al., 1975 ; Hill et al., 1981), in the Owase area in the Ki-i Peninsula (Takeda et al., 1976 ; Takeda and Takase, 1980), and in the Orofure mountain range in Hokkaido, Japan. It is generally accepted that the annual mean rainfall amount and the times of heavy rainfalls on Hokkaido Island are smaller than those in other districts in Japan. However, on the southeastern slope of the Orofure mountain range facing the Pacific Ocean in the southwestern part of Hokkaido, there is a relatively large annual mean rainfall, and heavy rainfalls amount to more than  $90 \text{ mm day}^{-1}$  three or four times per year (Takeda and Kikuchi, 1978). This area has been frequently subjected to floods and landslides arising from heavy rainfalls (Harimaya et al., 1981). If the mechanisms of heavy rainfalls are clarified, the flood and damage they result in could be reduced through adequate forecasts of rainfall.

Kikuchi and his group have studied the heavy rainfalls in this region since 1978. Konno and Kikuchi (1981) classified the horizontal distribution of rainfall amount into five types according to the locations where the maximum peak of rainfall amount was located based on the results of observations using their special mesoscale raingauge network. They clarified that the distribution patterns were mainly influenced by the wind direction in the lower layer. Konno et al. (1981) made the observations on the size distribution of raindrops at two observation sites simultaneously in the mountain range and at the seaside of the same area. The results of their observations suggested that the heavy orographic rainfalls in this range arose from a combination of lower layer clouds caused by an uplifting of the warm and wet air from the Pacific Ocean on the southeastern slope of the range and the precipitation from the upper layer clouds of the synoptic scale disturbance moving from the southwest to the northeast over this region. The numerical experiments by Konno and Kikuchi (1981) and Kikuchi et al. (1988) supported this conclusion and Iwanami et al. (1988) clarified the enhancement of the rainfall amount by the two-layer cloud structure model (Bergeron, 1965) through their radar observation.

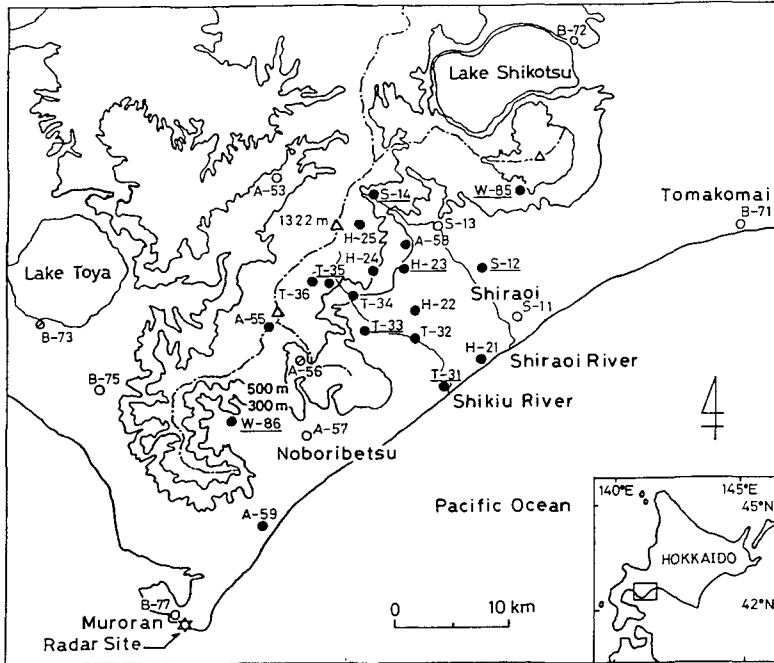


Fig.1. Map of the observation area and arrangement of instruments. Contour curves have been drawn for 300 and 500 m a.s.l. The curving chained lines represent crestlines. Symbols of observation sites—○: meteorological observatory and AMeDAS supported by JMA, ⊙: rainfall amount measuring robot supported by JMA, ●: rain gauge supported by this work. Wind vanes and anemometers were set up at the sites underlined and microbarometers at S-11, S-13 and T-32.

Kikuchi et al. (1988) further pointed out the importance of the role of the horizontal convergence in the increase of rainfall amounts on the mountainous regions because the valley became narrower from the seaside to the mountain side. This was noted in the results of their observations and numerical experiments. Tobizuka and Harimaya (1989) made a case study of seaside rainfalls in which the maximum peak of rainfall amount was located in the seaside region. It was shown that seaside rainfall was formed through a process in which echo cells, because of the discontinuity in the surface roughness, developed rapidly on the southeastern slope after crossing over the ridge of the range by frictional convergence. Iwanami et al. (1989) also reported seaside rainfall from the shallow convective precipitating clouds with echo tops lower than 3 km formed by a southeasterly flow of outbreak from the high pressure over the Okhotsk Sea. Iwanami et al. (1997a) reported the heavy rainfall case where

passing of an internal gravity wave was one of the mechanisms which enhanced rainfall amount.

In this paper, we describe the results of case studies of two heavy rainfall cases that contrasted with each other. One was caused by the stratiform precipitation clouds from 3 to 4 September 1986 and the other by convective precipitation clouds from 10 to 11 September 1986 associated with synoptic scale disturbances in the Orofure mountain range in Hokkaido, Japan.

## 2. Observations

Our radar observations of rainfalls were carried out in the Orofure mountain range from late August to early September for about 3 weeks in 1985 and 1986, using a combination of raingauges, wind vanes and anemometers, and microbarometers. Figure 1 shows the observation area and arrangement of instruments. The southeastern slope of the Orofure mountain range running nearly parallel to the coastline faces the Pacific Ocean from Tomakomai (tentative site number of our observations: B-71) through Shiraoi (S-11), Noboribetsu (A-57) to Muroran (B-77), thus the orographic rainfalls caused by the orographic uplifting of the warm and wet southeasterly airflow from the Pacific Ocean occur frequently in this area. In the figure, the locations of the meteorological observatories, AMeDAS and the rainfall amount measuring robots supported by the Japan Meteorological Agency (JMA), and of our 17 sites of raingauge of the tipping bucket long period automatic type (CMO-LRT 55) are represented by their respective symbols. The locations of almost all raingauge sites were the same as that of the past observations (Konno and Kikuchi, 1981; Kikuchi et al., 1988). Further we set up 7 wind vanes and anemometers at the sites underlined to research for the first time in the observations in this area, the airflow near the ground surface and 3 microbarometers (PD80HA, ST LAB., INC.) at S-11, S-13 and T-32 to investigate the relationship between convective activity and the perturbation of surface air pressure. A wind vane and anemometer at W-85 (without a raingauge) and a microbarometer at S-11 were set up in 1985. Raingauges at A-59 and W-86 and wind vanes and anemometers at T-33 and W-86 in 1986 were used to collect more data in the southwestern part of this area.

This observation network includes two valleys; the S-line along the Shiraoi River from Shiraoi (S-11) to the Shiraoi waterfall (S-14), and the T-line along the Shikiu River from Takeura (T-31) to close to the watershed of Kushibetsu (T-36). The H-line from Hagino (H-21) to near Todomatsuzawa

(H-25) was located on the ridge between the two lines described above. The A-53 site (Ohtaki-AMeDAS by JMA) is located on the northwestern slope of the Orofure mountain range.

The mobile weather radar of the Faculty of Science, Hokkaido University was set up on a cliff (118 m above the sea level) on the southeast side of Muroran City in order that the southeastern slope of the Orofure mountain range be watched from that side in consideration of observation results in 1983 (Tobizuka and Harimaya, 1989). The radar had a 9,410 MHz frequency, 30 kW peak transmitting power and resolution of 250 m in radial and 1.0 degree in azimuthal direction. It was connected with a data processor and three-dimensional digital data of precipitating clouds within 63.5 km range in radius could be obtained by volume scans consisting of several PPI (Plan Position Indicator) scans with an elevation angle interval of 1.1 degree every 10 minutes. The data were recorded on magnetic tapes after the range correction, data averaging, and the elimination of the ground clutter by the non-coherent MTI (Moving Target Indicator) method. Therefore, the distributions of the radar reflectivity factor could be displayed on PPI and CAPPI (Constant Altitude PPI) with 1 km  $\times$  1 km grids and on the arbitrary vertical cross section with 1 km (horizontal)  $\times$  0.5 km (vertical) grids in time of analyses. The RHI (Range Height Indicator) scan was also available and the data were recorded on floppy disks in 1986.

### 3. Results

#### 3.1 *Heavy rainfalls from stratiform precipitation clouds*

Heavy rainfalls were caused by the stratiform precipitation clouds which passed over the observation area from September 3 to 4 in 1986. The surface wind direction at the S-11 site was not typically southeasterly for the heavy rainfalls in this area but rather north-northeasterly, and our attention was focused on two ridges stretching southeastward near Noboribetsu City.

The horizontal distribution of the total rainfall amount for this case is shown in Fig. 2. The rainfall amount was distributed over a wide area not only on the southeastern slope of the Orofure mountain range but also on the northwestern slope of that range. The widespread distribution of the rainfall amount is a feature of rainfalls in this area when associated with surface winds of northerly to north-northeasterly. The maximum peak was located near the crestline, and the H-25 site recorded 169 mm for 21 hours. The rainfall amount along the T-line, which was located northeastward of the ridge stretching southeastward, was distinctively more than that on the far eastward side.

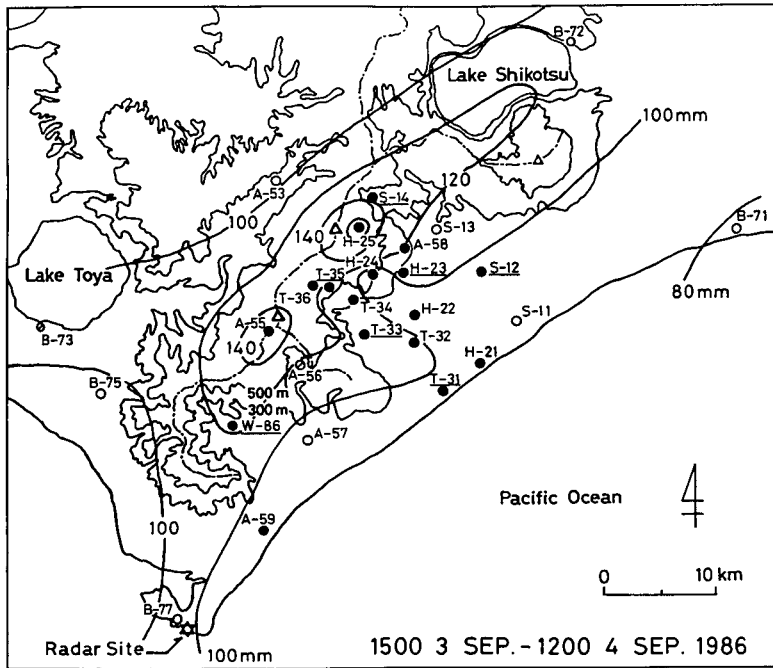


Fig. 2. Horizontal distribution of total rainfall amount from 15 JST on September 3 to 12 JST on September 4, 1986. Contours of rainfall amount are drawn at 20 mm intervals from 80 mm.

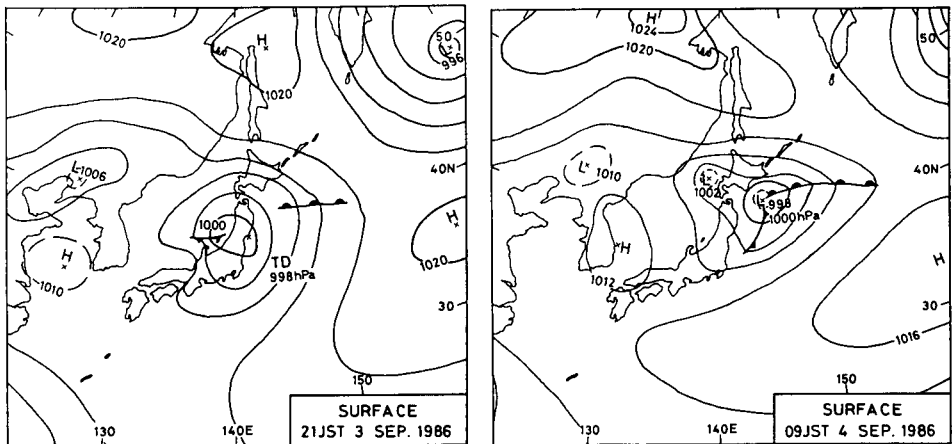


Fig. 3. Surface weather charts at 21 JST on September 3 and 09 JST on September 4, 1986.

The surface weather charts at 21 JST on September 3 and 09 JST on September 4 in 1986 are shown in Fig. 3. The tropical depression traveling northward existed above Sendai (21 JST on Sep. 3) and moved over the Pacific Ocean, then reached offshore Kushiro and changed to the extratropical cyclone (09 JST on Sep. 4). A sub-depression has generated off Shakotan Peninsula and the northerly wind was blowing into the main depression off Kushiro over Hokkaido Island. Judging from the aerological data of Sapporo at 21 JST on September 4, the  $0^{\circ}\text{C}$  level was 4.7 km a.s.l. and the relative humidity was more than 80% extended from the ground level to the height of 7.5 km. Convective unstable layers existed from the ground surface to about 700 m and from 2.4 to 3.9 km.

Figure 4 shows the time series of the rainfall intensities per 20 minutes at the S-14, H-25, A-55 and W-86 sites that recorded more than 120 mm of their total rainfall amounts. The rainfalls continued from about 16 JST on Septem-

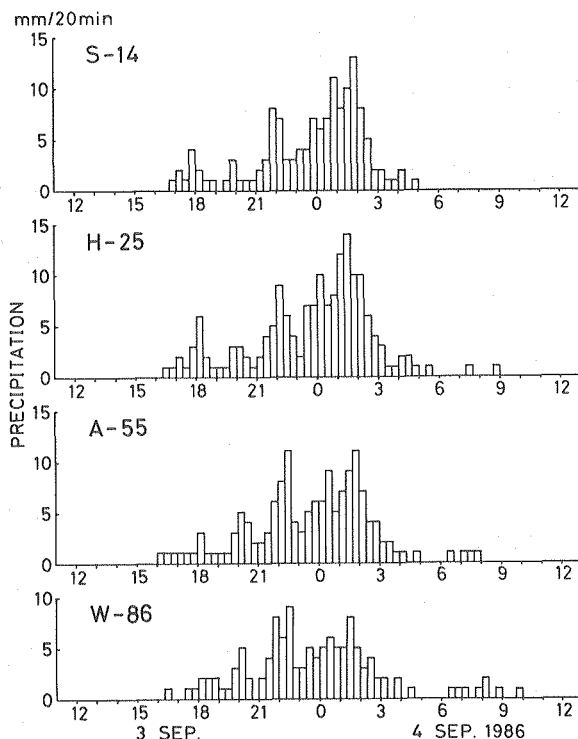


Fig. 4. Time series of rainfall intensity per 20 min at the sites of S-14, H-25, A-55 and W-86.

ber 3 to about 05 JST on September 4 at these sites and others. There were about five peaks at each site, however the rainfall period was divided into two parts from the radar echo analysis. The bright band was remarkable in the first half before 21 JST on September 3 when rainfall intensity was weak, and in the second half the convective activity in the lower layer was comparatively strong and a rainfall intensity of more than 10 mm per 20 minutes was recorded.

In the first half of this rainfall period, radar echoes were stratiform and considerably uniform. Figure 5 shows CAPPI pictures of 2.0 and 5.0 km a.s.l. calculated by the PPI series recorded from 18:30 to 18:37 JST on September 3, 1986. The echoes stronger than 20 dBZ spread over a wide area of about 100 km $\times$ 50 km above the radar site on the 5.0 km CAPPI picture that seemed to correspond to the bright band. On the 2.0 km CAPPI, the echoes in the lower layer had comparatively uniform reflectivity weaker than 25 dBZ below the bright band area shown in 5.0 km CAPPI and no developed echo was observed over the southeastern slope of the Orofuro mountain range. On the corresponding RHI pictures over the mountainous region at the azimuth of 29.7 degree (line O-P in Fig. 5) and along the coastline of 47.5 degree (line O-Q in Fig. 5), two layers with echoes stronger than 25 dBZ existed at around 4.8 km and below 2.0 km a.g.l. (the radar site at 118 m a.s.l.). Since the 0°C level was 4.7 km a.s.l. according to the aerological data at Sapporo, it is considered that the precipita-

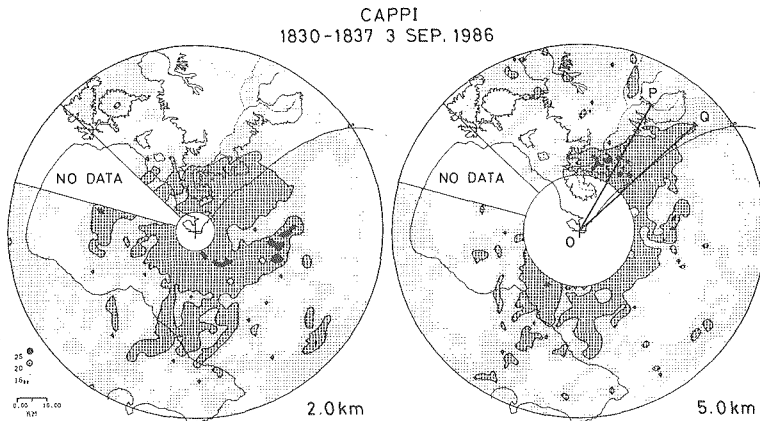


Fig. 5. CAPPI pictures at 2.0 km (left) and 5.0 km (right) a.s.l. for 18:30-18:37 JST on September 3, 1986. Echo intensities are shown by both contours and symbols indicated on the lower left of the figure. The outer and inner circles of each panel show maximum range of 63.5 km and no data areas. Coastline, crestline and contours of 300 m a.s.l. are drawn by slightly thick solid, thin dashed and thin solid lines, respectively.

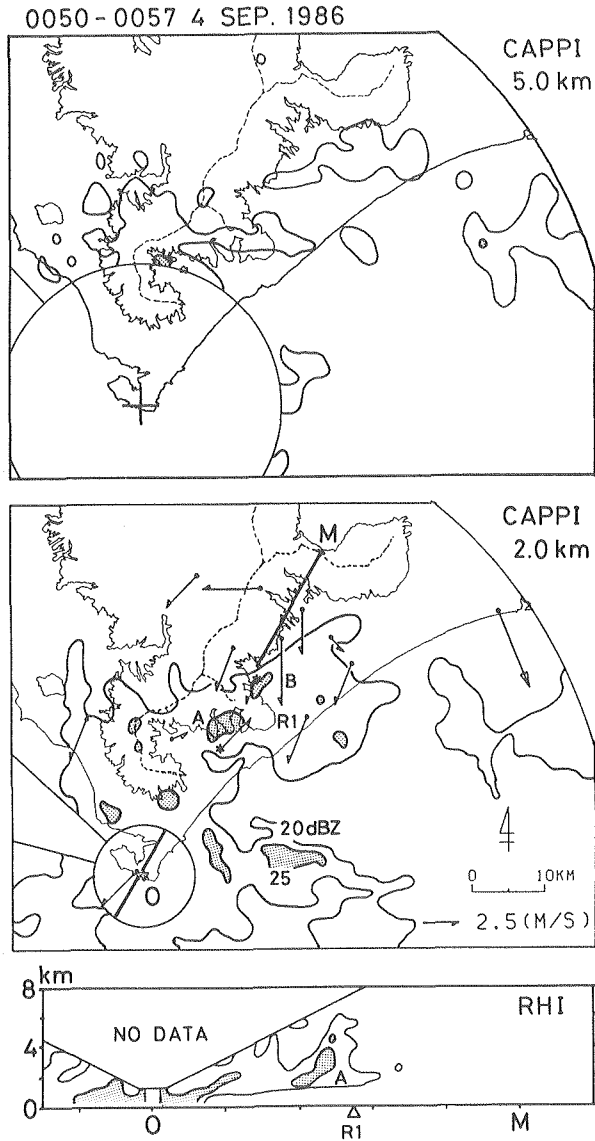


Fig. 6. CAPPI pictures of 5.0 km (top) and 2.0 km (middle) a.s.l., and vertical cross section (RHI; bottom) along the line O-M drawn by thick solid line in 2.0 km CAPPI for 00:50-00:57 JST on September 4, 1986. Surface wind field for 00:50-01:00 JST is superimposed on 2.0 km CAPPI. Contours of echo intensities are drawn for 20 and 25 dBZ and the echo areas stronger than 25 dBZ are stippled. Coastline (slightly thick solid line), crestline (thin dashed line) and contours of 300 m a.s.l. (thin solid lines) are also drawn. Winds are indicated by arrows, and the A-57 and T-33 sites are denoted by asterisks. The small open triangle with the horizontal axis of the vertical cross section (RHI) denotes the location of the ridge R1 stretching southeastward.

tion particles in the ice phase falling from the upper level began to melt and made the bright band at around 4.8 km a.s.l., and that they further continued to fall and grew to larger raindrops through collision and coalescence processes in a very humid lower layer and formed the thin and strong echo layer below 2.0 km a.s.l.

The surface winds on the southeastern slope of the Orofure mountain range were almost northerly and weak in the first half period, and it is therefore considered that the effects of topography on the precipitation clouds did not appear over this area. However the surface winds at the A-57 and W-86 sites changed into a southerly direction from 23 JST on September 3 in the second half period and the radar echoes in the lower layer developed around two ridges stretching southeastward.

Figure 6 represents the 5.0 km CAPPI picture, and the 2.0 km CAPPI picture superimposed with surface wind distributions. The vertical cross section (RHI) along the line O-M indicated in 2.0 km CAPPI is also shown. The CAPPI pictures and vertical cross section were constructed from the PPI series recorded at 00:50-00:57 JST and the surface winds were 10 min average values for 00:50-01:00 JST on September 4. Developed echoes of A and B stronger than 25 dBZ existed over the southwestern and northeastern slopes of the ridge R1 stretching southeastward on 2.0 km CAPPI. The surface winds at the A-57 and T-33 sites (indicated by asterisks) situated on both sides of this ridge were southwesterly and north-northeasterly, respectively. Although the contours of 16 dBZ are omitted for simplicity's sake, the echo areas stronger than 20 dBZ indicated in the figures were surrounded by wide echo areas with reflectivities ranging from 16 to 20 dBZ. The echo intensity was comparatively uniform in the upper layer on the 5.0 km CAPPI picture and the difference in the amount of falling precipitation particles was assumed to be small. It is considered therefore that the strong echoes in the lower layer over the ridge R1 stretching southeastward were developed by the updrafts along the slopes of the ridge blown by the winds near the ground surface. This developed echo A is also found on the vertical cross section (RHI) near the ridge R1 indicated by a small open triangle.

In Fig. 7, 10 minutes later, the surface wind direction at the A-57 site changed from southwest to east-northeast and the radar echo C in the lower layer developed over the northeastern slope of the ridge R2 at the southwest end of the mountain range to which the surface wind was blowing. This developed echo C also appears northward to the ridge R2 indicated by the small solid triangle on the vertical cross section along line O-N.

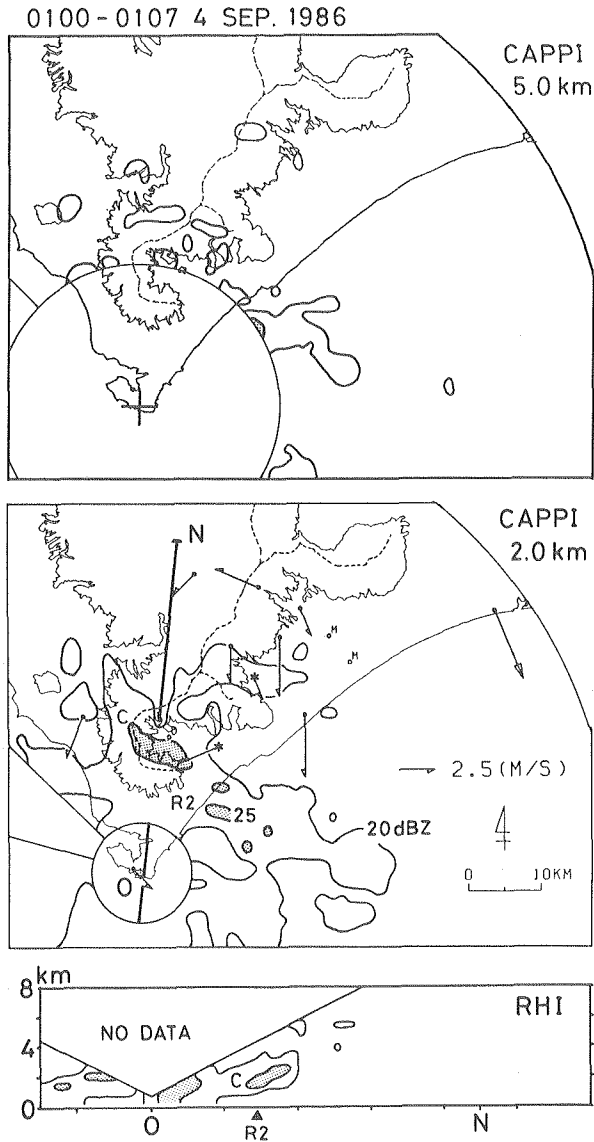


Fig. 7. As in Fig. 6, but for CAPPI pictures and vertical cross section (RHI) along the line O-N drawn in 2.0 km CAPPI for 01 : 00-01 : 07 JST and the surface wind field for 01 : 00-01 : 10 JST on September 4, 1986. The location of the ridge R2 on the line O-N is represented by the small solid triangle on the vertical cross section.

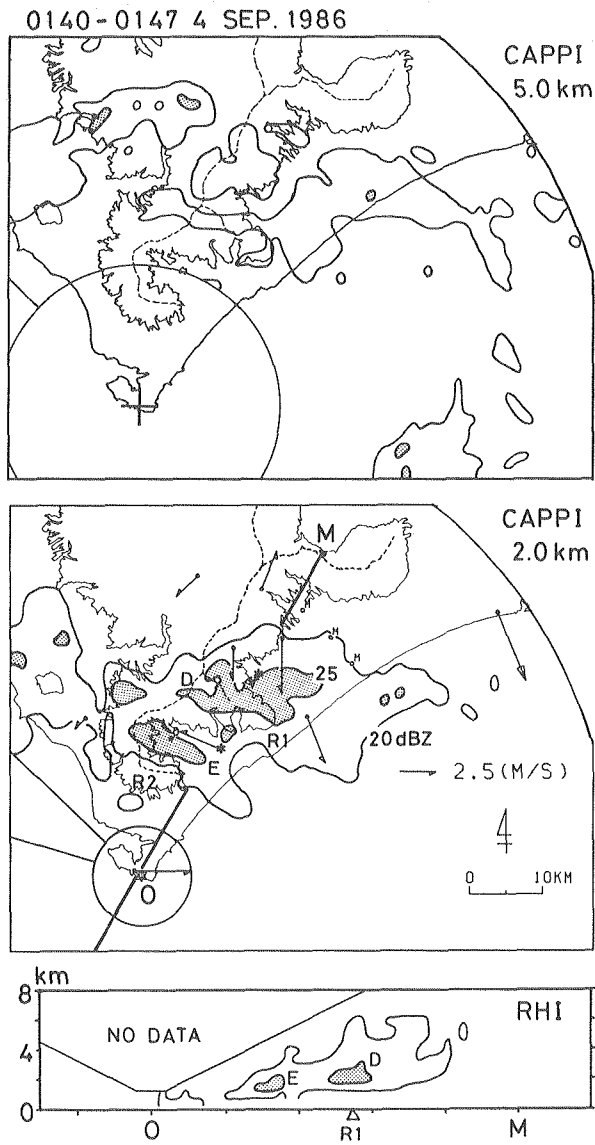


Fig. 8. As in Fig. 6, but for CAPPI pictures and vertical cross section (RHI) for 01 : 40-01 : 47 JST and the surface wind field for 01 : 40-01 : 50 JST on September 4, 1986.

The surface winds remained northerly on the northeast side and southerly on the southwest side of the ridge R1 after 01 JST on September 4. Figure 8 shows the distribution of the radar echoes for 01:40-01:47 JST and surface winds for 01:40-01:50 JST as in Fig. 6. The echoes from 20 to 25 dBZ in reflectivity in the upper layer on 5.0 km CAPPI passed northeastward over this area, however the developed echo D, which was stronger than 25 dBZ in the lower layer on 2.0 km CAPPI, stayed over the ridge R1. The ridge stretching southeastward was blown by northerly surface winds. The developed echo E over the northeastern slope of the ridge R2 seemed to be produced by west-southwesterly winds as surmised by the A-57 winds.

Figure 9 shows a time series of the vertical cross section (RHI) along the line O-M drawn in 2.0 km CAPPI of Fig. 8 at 10 min intervals from 01:00 to 02:10:

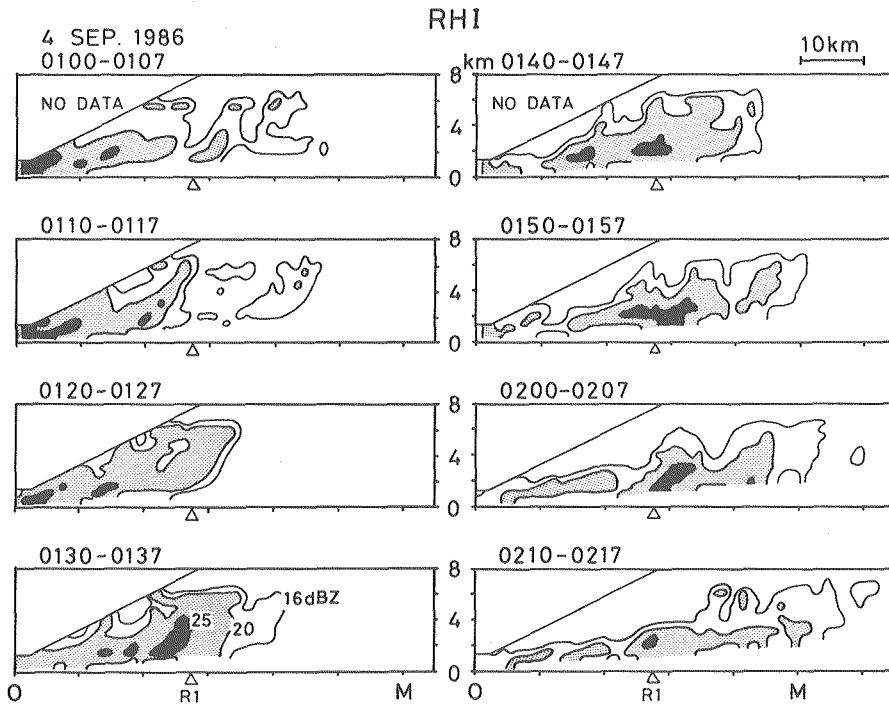


Fig. 9. Time series of vertical cross sections (RHI) along the line O-M drawn by thick solid line in the 2.0 km CAPPI in Fig. 8 at 10 min intervals from 01:00-01:07 to 02:10-02:17 JST on September 4, 1986. Contours of echo intensities are drawn for 16, 20 and 25 dBZ and the echo areas stronger than 20 and 25 dBZ are stippled and blacked out, respectively. The small open triangle with the horizontal axis of each cross section denotes the location of the ridge R1 stretching southeastward.

10 JST on September 4. The open triangle of each panel indicates the location of the ridge R1 stretching southeastward. The stratiform echoes weaker than 25 dBZ in the upper layer below 6.0 km a.s.l. passed successively over this area, however in the lower layer the developed echoes stronger than 25 dBZ stayed generally over the ridge R1 especially after 01:30 JST. The large rainfall amount around this ridge as compared with that on the surrounding region as previously described in the Fig. 2 was considered to be caused by the developed precipitation clouds in the lower layer. It is therefore concluded that the topography produced these small scale effects on the stratiform precipitation clouds passing over the observation area.

### 3.2 Heavy rainfalls from convective precipitation clouds

In contrast to the case described in the previous section, the rainfalls on September 10 to 11 in 1986 were caused by the developed convective precipitation clouds whose echo top reached higher than 10 km a.s.l. In addition, a

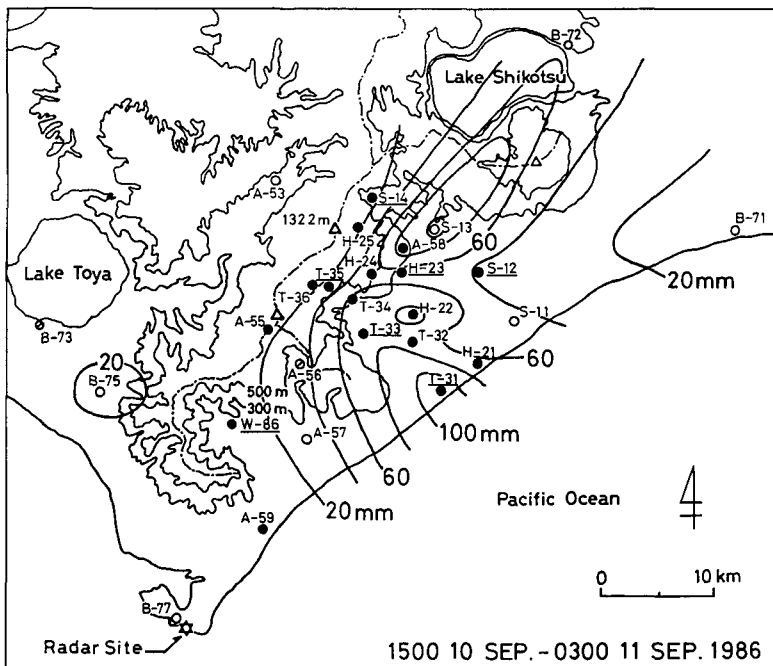


Fig. 10. Horizontal distribution of rainfall amount for 12 hours from 15 JST on September 10 to 03 JST on September 11, 1986. Contours of rainfall amount are drawn at 20 mm intervals from 20 mm.

rainfall intensity of  $108 \text{ mmhr}^{-1}$  was recorded at the T-31 site from 23 to 24 JST on September 10, 1986.

The total rainfall amount at the sites of T-31, S-13 and A-58 exceeded 140 mm for this case from 23 JST on September 9 to 08 JST on September 11. Figure 10 shows the rainfall amount distribution through an interesting 12 hour period. The rainfall amount was limited to the southeastern slope of the Orofure mountain range. There were three peaks of rainfall amount : in the mountainous region around the S-13 ; in the plain region around the H-22 ; and

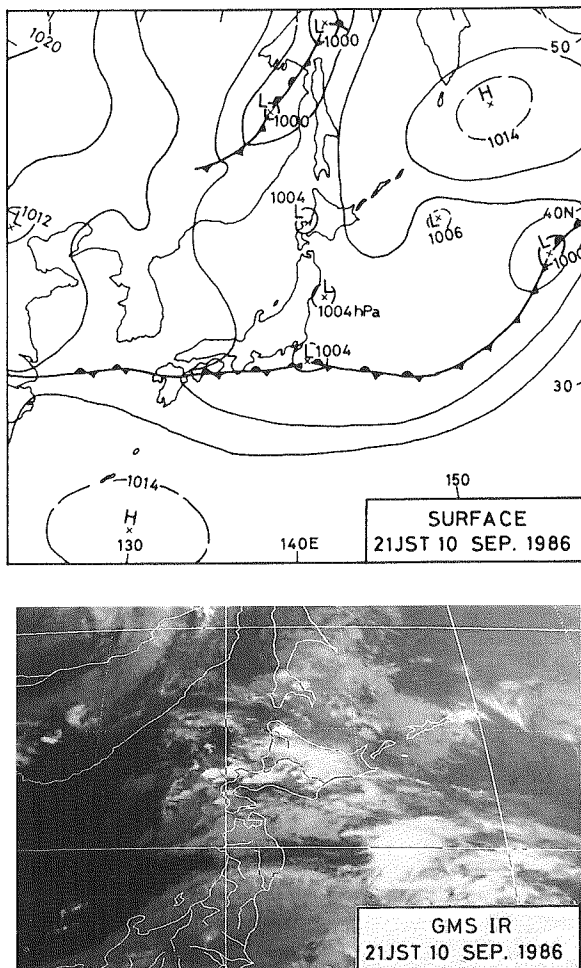


Fig. 11. Surface weather chart and IR image of GMS at 21 JST on September 10, 1986.

on the seaside region centered on the T-31 site. The rainfall amounts for 1 hour from 23 to 24 JST on September 10 at the T-31 and H-21 sites in the seaside region were 108 and 60 mm, respectively, and they accounted for 12 hr rainfall amounts from 15 JST on September 10 to 03 JST on September 11.

The surface weather chart and IR image of GMS at 21 JST on September 10 in 1986 are shown in Fig. 11. The trough traveling eastward covered the northern part of Japan and the atmosphere over Hokkaido Island became unstable because of the inflow of a warm and moist air mass. The southerly wind blowing into the depression that moved above Otaru was predominant over the observation area after about 08 JST on September 10, so deep clouds, that were considered to correspond to the radar echoes shown near the observation area are recognized on the IR image. A vertical profile of the equivalent potential temperature in Sapporo at the same time is shown in Fig. 12. It indicates that the convective unstable or nearly neutral layers extended to the

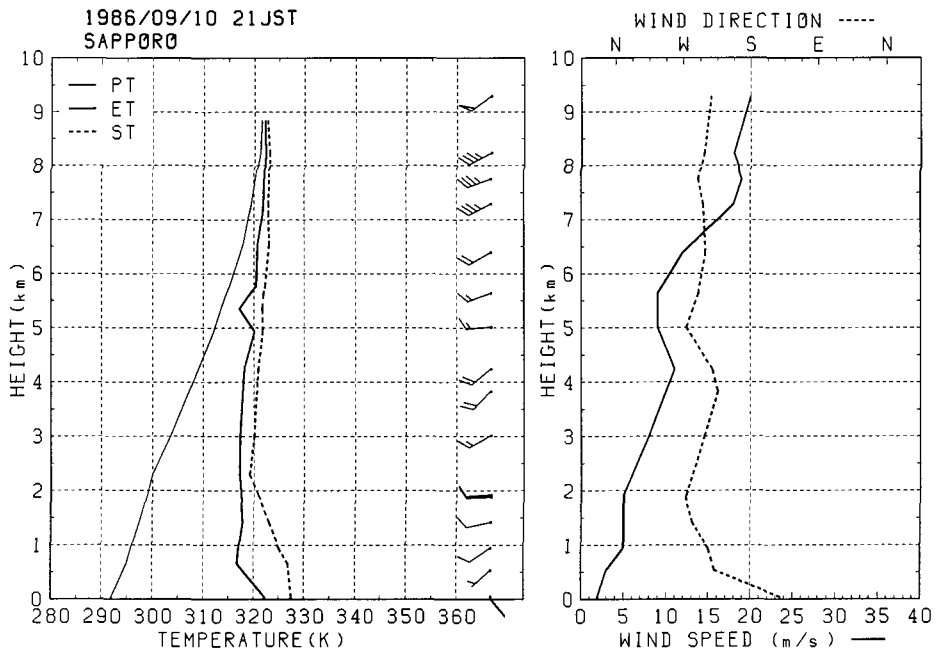


Fig. 12. Left panel: Vertical profiles of potential temperature (thin solid line), equivalent potential temperature (thick solid line) and saturated equivalent potential temperature (dashed line) at Sapporo. Wind velocities are also indicated by flag (20 ms<sup>-1</sup>), full barb (5 ms<sup>-1</sup>) and half barb (2.5 ms<sup>-1</sup>). Right panel: Vertical profiles of wind direction (dashed line) and speed (solid line) above Sapporo at 21 JST on September 10, 1986.

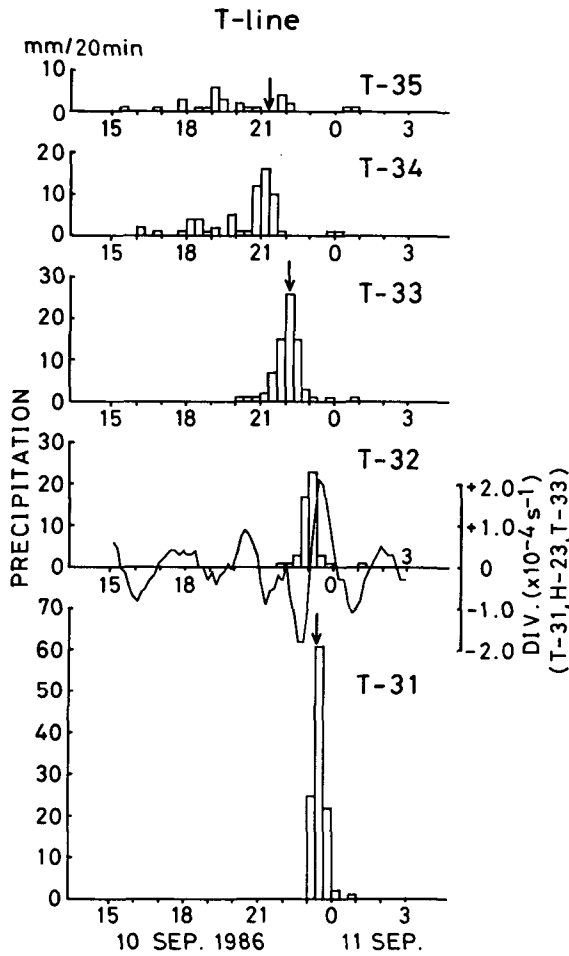


Fig. 13. Time series of rainfall intensity per 20 min at the sites along the T-line. The times of wind shifts are indicated by arrows, and time evolution of surface divergence deviation from the 3-hour running mean are shown.

far upper level and the atmosphere was suitable for severe convective activity.

Figure 13 shows a time series of the rainfall intensity per 20 minutes at the five raingauge sites along the T-line. These time series are arranged from the seaside to the mountainous region upward from the bottom of the figure. The weak rainfalls before about 20 JST on September 10 were recorded only at the sites in the mountainous region, and from 21 to 24 JST the raingauge sites that recorded the intense rainfalls more than 10 mm per 20 minutes turned from the

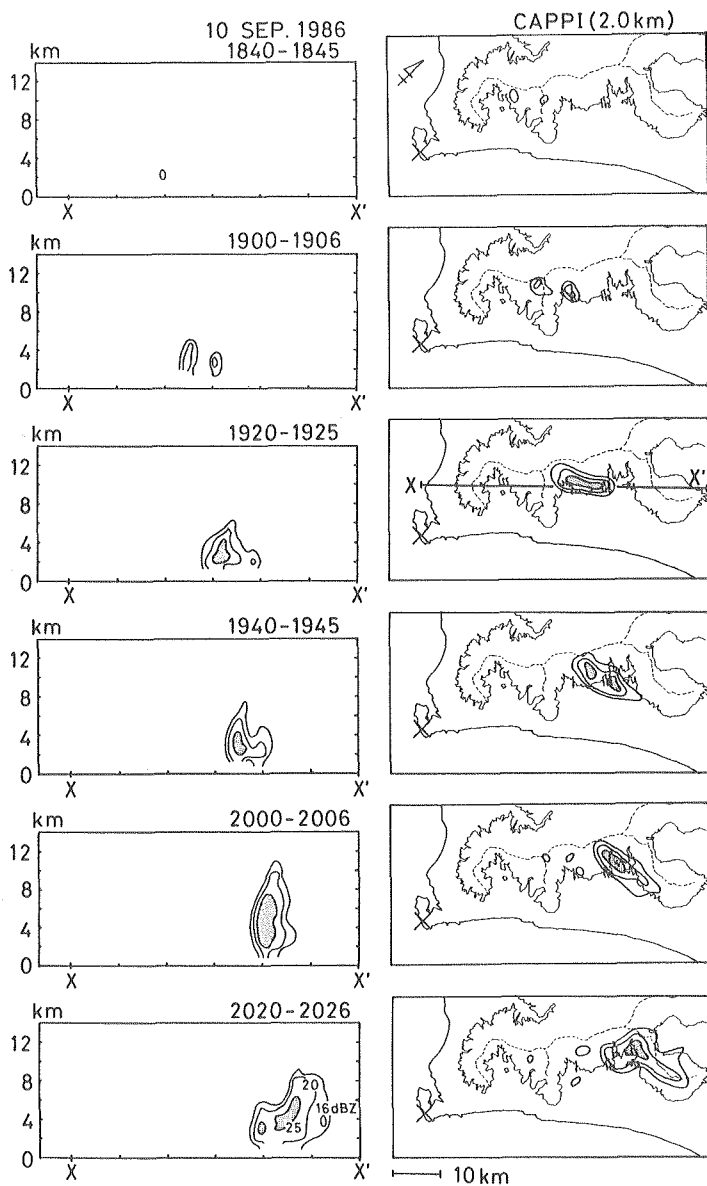


Fig. 14. Time series of CAPPI pictures at 2.0 km a.s.l. (right) and the vertical cross sections (left) along the line X-X' drawn by the thick solid line in the third CAPPI at 20 min intervals. The first contour of the echo indicates 16 dBZ and the contours of echo intensity are drawn at 5 dBZ intervals from 20 dBZ, and the echo areas stronger than 25 and 35 dBZ are stippled and blacked out, respectively. Coastline, crestline and contours of 300 m a.s.l. in the 2.0 km CAPPI are drawn by slightly thick solid, thin dashed and thin solid lines, respectively. Note that the north is directed to upper right in 2.0 km CAPPI pictures.

T-34 in the mountainous region to the T-31 site in the seaside region. This intense rainfall was caused by band-shaped deep convective precipitation clouds. These precipitation clouds were traced by the radar echo analysis.

Figures 14 to 17 show the time series of the CAPPI pictures at 2.0 km a.s.l. and vertical cross sections at 20 min intervals. These CAPPI pictures and vertical cross sections were calculated from the PPI series recorded for the period indicated with respective pictures. These CAPPI pictures should be viewed with the north directed to upper right. In Fig. 14, vertical cross sections were constructed along the direction of the echo movement (X-X'). The echo cells were generated near the crestline of the southwestern part of the observation area at 18:40 JST and moved northeastward in parallel with the mountain range. They developed into echoes with reflectivity more than 25 dBZ and with the top height of 11 km a.s.l. at 20:00 JST in the mountainous region of the northeastern part of this area. The rainfalls in the mountainous region as shown in Fig. 13 resulted from the passage of these precipitation clouds. Southerly winds from the Pacific Ocean blew over the southeastern slope of this mountain range during this period, and it is considered that the forced uplifting of the southerly flow in the convective unstable layer was one of the causes of the generation and development of these precipitation clouds in the mountainous region.

The new echo cells appeared near the crestline of the southwestern part of this area at 20:00, 20:20 JST shown in Fig. 14 and 20:30 JST in Fig. 15, and they traveled along the mountain range and developed. Judging from the aerological data at Sapporo, the wind direction at the 800 hPa level changed from southwest at 15 JST to west at 21 JST on September 10 and to west-northwest at 03 JST on September 11 associated with the movement of the depression. Probably corresponding to this change, after 20:50 JST the echoes began to move east-northeastward and the surface wind at the T-35 site changed from south-southeasterly to north-northeasterly at 21:20 JST. The location of the T-35 site is indicated by an asterisk in the CAPPI picture at 21:30 JST. The new cells were generated successively in the more southeastward mountainous region of the southwestern part of this area after 20:50 JST and they were organized into the band-shaped echo along Z-Z' line at 21:51 JST on September 10.

The vertical cross sections shown in Figs. 16 and 17 were constructed along the T-line (T-T') on the left side and along the direction of the band-shaped echoes (A-A' to D-D') on the right side of the figures, and small open and solid triangles indicate the locations of the crest and coast along the T-line, respec-

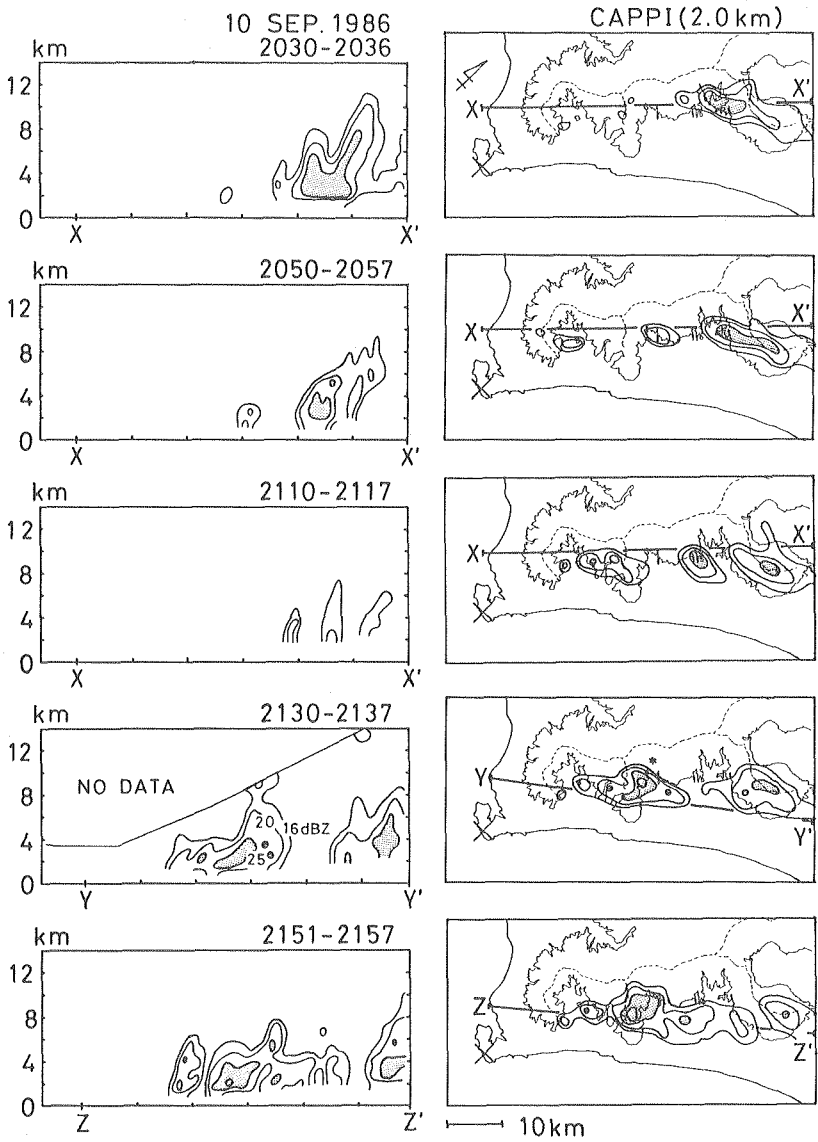


Fig. 15. As in Fig. 14, but for from 20:30 to 21:51 JST on September 10, 1986. The direction along which each vertical cross section was calculated is drawn by thick solid line in each corresponding CAPPI picture.

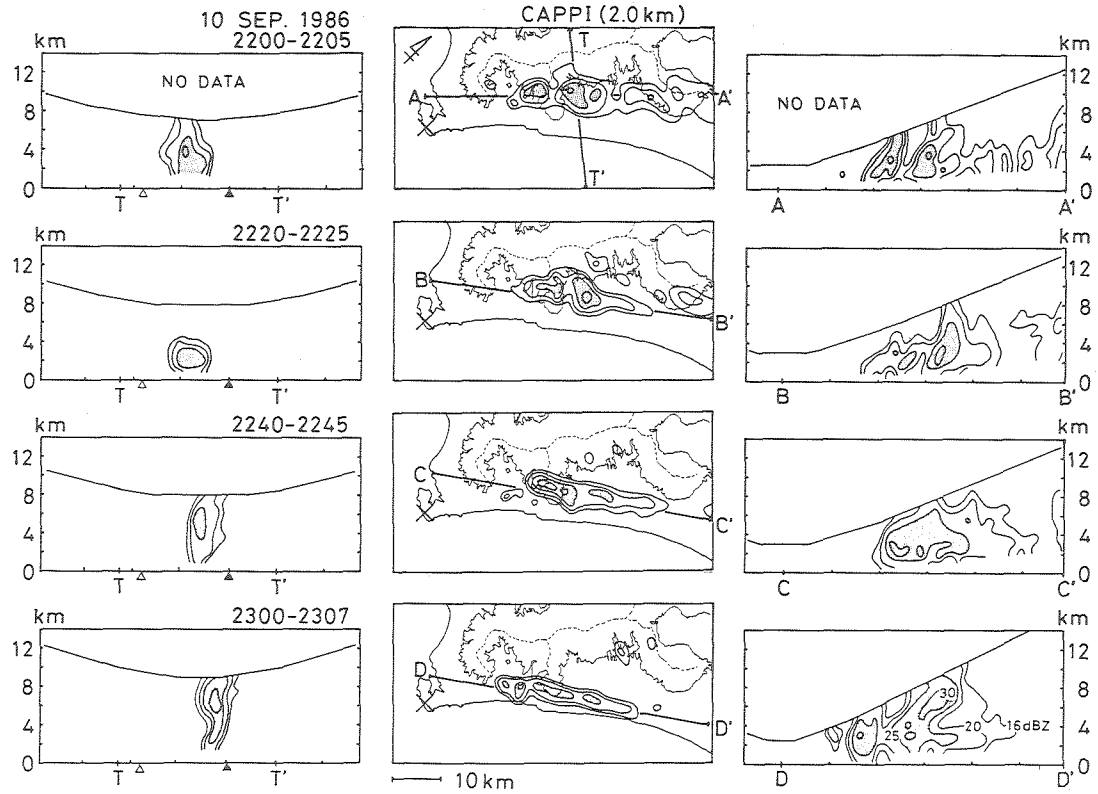


Fig. 16. Time series of the CAPPI pictures at 2.0 km a.s.l. (center column), the vertical cross sections along the T-line (T-T') indicated by the thick solid line in the first CAPPI picture (left) and along the directions drawn by the thick solid lines in the corresponding CAPPI pictures (right) at 20 min intervals. Other representations are the same as in Fig. 14.

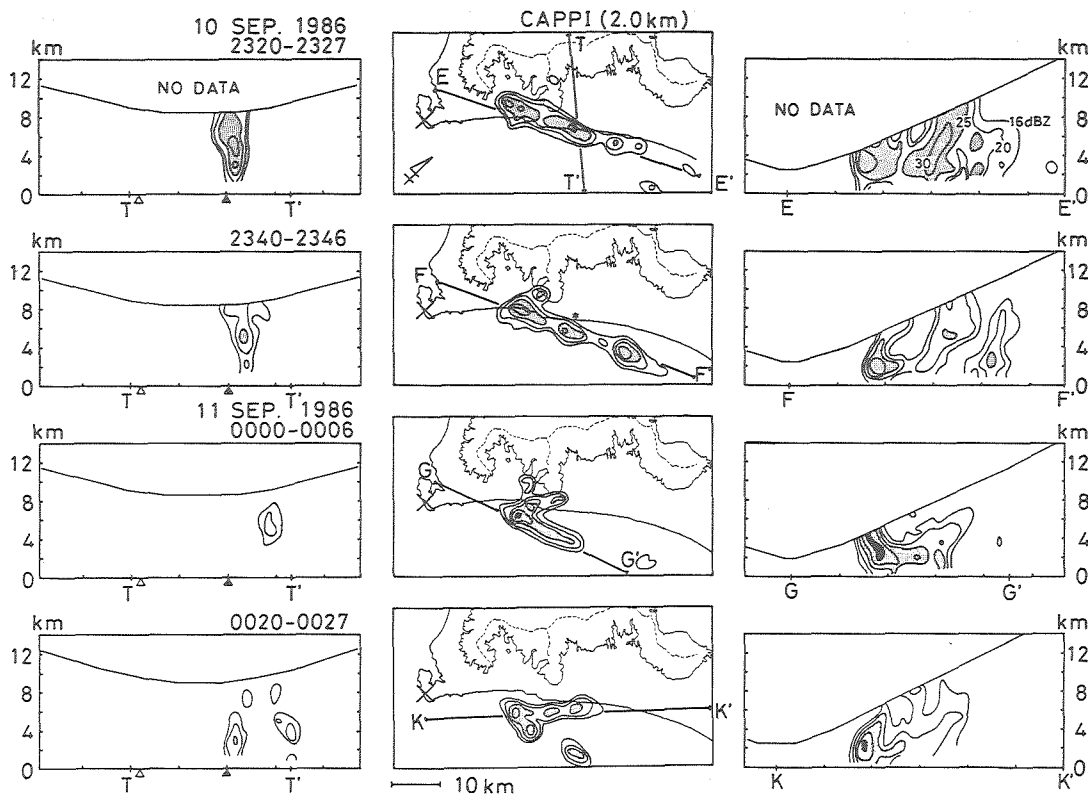


Fig. 17. As in Fig. 16, but for from 23:20 JST on September 10 to 00:20 JST on September 11, 1986.

tively. The surface wind at the T-33 site (indicated by an asterisk in the CAPPI at 22:40 JST) changed from southwesterly to northwesterly at 22:10 JST on September 10 although the surface wind at the T-31 site in the seaside region remained southerly. The band-shaped echo existed in the plain region as shown in Fig. 16 over the shear line formed between the northerly winds on the northwestern side and southerly winds on the seaward side. Each cell in this band-shaped echo moved to approximately eastward in this period and new cells were generated at the southwest end of this band-shaped echo that was the confluence of southerly winds in the lower layer from the sea with the divergent flow associated with the downdrafts caused by the rainfalls at 22:40 JST. The width of the band-shaped echo was growing narrower when it approached the coastline, then an echo had the form with width and length at about 5 and 30 km, respectively. The echo top reached higher than 10 km a.s.l. and the echo area stronger than 30 dBZ spread on the vertical cross sections at 23:00 JST on September 10.

The T-31 site (indicated by an asterisk in the CAPPI picture at 23:40 JST shown in Fig. 17) on the seaside region recorded a rainfall amount of 61 mm during 20 minutes for 23:20-23:40 JST and the surface wind at that site changed from southerly to northwesterly at 23:20 JST. The echo area stronger than 30 dBZ fell from 23:00 to 23:20 JST above the T-line, then very deep convective precipitation clouds passed over the seaside region as shown in Fig. 17. It is speculated that the echo top of these precipitation clouds reached about 12 km a.s.l. after considering the no data area on the vertical cross sections. These precipitation clouds moved over the sea at 00:20 JST on September 11, and thereafter the northeary surface winds spread all-over the southeastern slope of the mountain range.

Figure 13 represents the times of the change of the surface winds from southerly to northerly by arrows with the time series of rainfall intensity per 20 minutes at the sites along the T-line. It is seen that the heavy rainfalls at the T-34 to T-31 sites were recorded when the surface winds were northerly on the northwestern side and southerly on the seaward side to each raingauge site. The time evolution of the surface divergence deviation from a 3-hour running mean, shown in Fig. 13, was calculated for the triangle area including the T-32 site surrounded by the T-31, H-23 and T-33 sites by using 10 min average surface winds. The deviation values continued to be negative (convergence) from 21:00 to 23:00 JST and reached  $-2.0 \times 10^{-4} \text{ sec}^{-1}$ , then changed to the divergence at 23:10 JST on September 10. The surface divergence values (not deviation) also experienced a time change similar to the deviation values. The

wind shift on the T-33 and T-31 sites occurred at 22:10 and 23:20 JST respectively and the heavy rainfall was recorded at the T-32 site from 22:40 to 23:20 JST. It is therefore considered that the updrafts were caused by this convergence produced over the shear line between the northerly and southerly winds and they enhanced the rainfall amount, and that the following divergence resulted from the downdrafts associated with the heavy rainfalls.

#### 4. Discussion

The updrafts, to begin with, should exist for the development of the convective activity: condensation of water vapor, formation and growth of precipitation particles and occurrence of heavy rainfalls. In this chapter, therefore, the quantitative estimation of updrafts caused by several possible mechanisms over the southeastern slope of the Orofure mountain range is carried out and contributions are discussed based on the observation results and conclusions described in the previous chapter and the other papers.

Most cases of rainfalls are associated with synoptic scale disturbances in general and this was also true in this area during the observation periods. It is well known that the representative convergence and updraft accompanied with synoptic scale disturbances amount to the order of  $10^{-6} \text{ sec}^{-1}$  and  $0.01 \text{ ms}^{-1}$ , respectively (Matsumoto, 1974).

Rainfalls produced by the forced uplifting over orographic regions have been extensively investigated to date (e.g., Sarker, 1966; Browning et al., 1974). Sawyer (1952) stated that the most striking feature of the rainfall distributions was the result of orographic lifting through two case studies carried out in the British Isles.

The wind field over the Orofure mountain range was estimated as the potential flow by Nakatsugawa et al. (1990). They calculated it as follows: first they constructed the digital map from the contour map of the analysis area and transformed topographic data into frequency components by the FFT (Fast Fourier Transform) method; next the FFT data were incorporated into the discrete solutions of the three-dimensional Laplace equation to derive the potential flow. Figure 18 represents the horizontal and vertical distributions of updrafts and it was drawn up for this work by using their calculation results presented by courtesy of them. The horizontal and vertical grid intervals are 2.0 and 0.2 km, respectively, and the calculation domain of  $63.8 \times 63.8 \text{ km}$  includes the Orofure mountain range. The upper boundary was set up at 5.0 km a.s.l. and the uniform southeasterly flow was inputted over the domain.

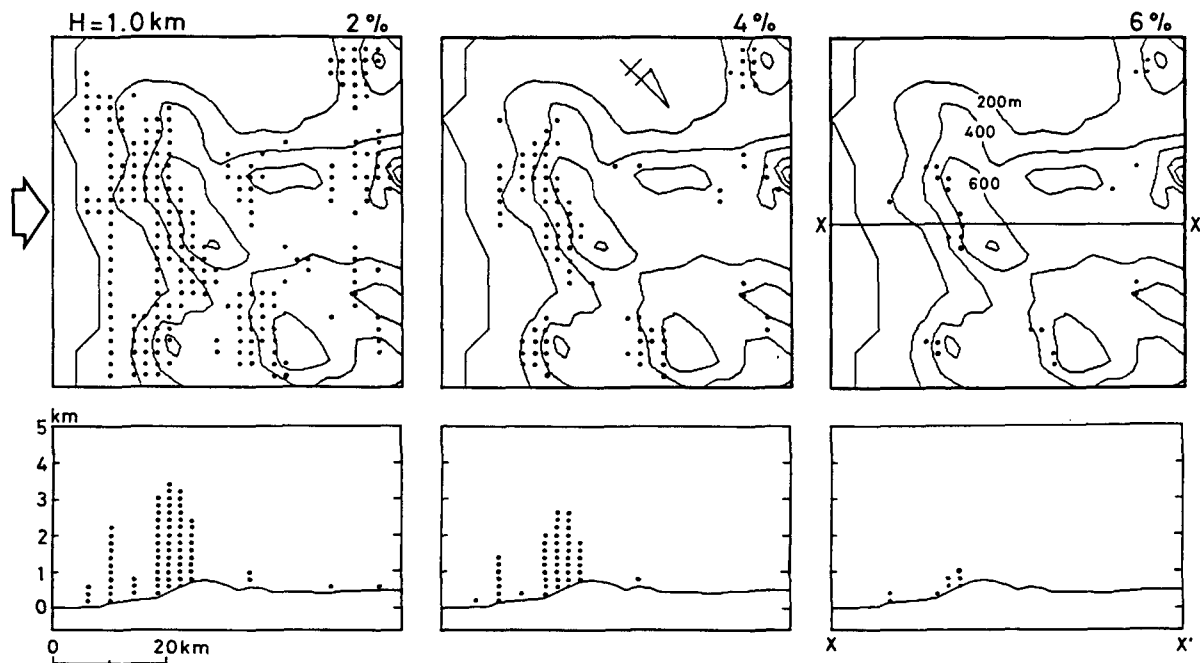


Fig. 18. Top: Horizontal distributions of updrafts at the 1.0 km a.s.l. level. Simplified coastline and contours of topography at 200 m intervals from 200 m are drawn. Note that the north is directed to lower right. Bottom: Vertical distributions of updrafts along the line of X-X' drawn in the top right panel. Dotted areas indicate the regions where the updrafts more than 2 (left), 4 (center) and 6% (right) of inputted southeasterly wind speed (broad open arrow) are estimated. (Constructed after calculation results by Nakatsugawa et al., 1990.)

The dotted areas in Fig. 18 demonstrate updraft regions where updrafts more than 2, 4 and 6% of inputted southeasterly wind speed were derived. It is seen that the updraft areas are distributed over the southeastern slope of the Orofure mountain range from the horizontal distribution at 1.0 km a.s.l. (top), and they extend to about 3.5 km a.s.l. over the slope on the vertical cross section (bottom). It is considered that the estimated updrafts caused development of radar echoes in the lower layer of the region between the two ridges stretching southeastward described in the section 3.1, and that they caused generation and development of precipitation clouds in the mountainous region described in the section 3.2. Further it is demonstrated that updraft areas are distributed near the coastline in the southwestern part of the southeastern slope although they are relatively limited near the ridge in the northeastern part of the slope seen on the top center panel indicating 4% updrafts. It seems that this feature corresponds to the observation results that shallow convective precipitation clouds were formed over the seaside region around Noboribetsu City in the rainfall case described by Iwanami et al. (1989) and over the middle of the slope in the case shown in the report by Iwanami et al. (1988).

The representative southeasterly wind speed to be inputted into the model was regarded, in consideration of the aerological data at Sapporo, as about  $10 \text{ ms}^{-1}$  over the observation area when heavy rainfalls occurred. Therefore the typical updraft values caused by the forced uplifiting are assumed to be  $0.2$  to  $0.6 \text{ ms}^{-1}$  because of the linearity of the potential flow model.

The horizontal convergence of airflow near the ground surface is one of the formation mechanisms of the updraft that is mainly caused by orographic features such as valleys. Kikuchi et al. (1988), through their numerical simulations, emphasized the importance of the role of the horizontal convergence in increasing the rainfall amounts on the mountainous region. Observed values of horizontal convergence using 10 min mean surface winds ranged from  $(1.5 \text{ to } 3.0) \times 10^{-4} \text{ sec}^{-1}$  described by Iwanami et al. (1989), and similar values were also observed in other rainfall cases. The surface convergence values associated with the shear line described in the section 3.2 also reached to about  $2.0 \times 10^{-4} \text{ sec}^{-1}$ . Assuming that this convergence remained up to a several hundred meter altitude above the ground surface, the updrafts caused by this surface convergence were estimated about  $0.1$  to  $0.2 \text{ ms}^{-1}$ , which were larger than those associated with synoptic scale disturbances.

The coastline generally represents a marked discontinuity in surface roughness. The resulting mechanical forcing leads to a secondary circulation in the boundary layer, and consequently to a vertical motion field that may have a

strong influence on the weather in the coastal zone. In convectively unstable air masses, frictional convergence may cause a more or less stationary zone of heavy rainfall activity. Roeloffzen et al. (1986) presented a calculation of secondary flow patterns forced at a roughness discontinuity. They also showed an example of heavy shower activity in the coastal zone of Belgium and the Netherlands, which was apparently due to frictional uplift and frontogenesis in a maritime polar air mass hitting the coastline. It is considered that the updrafts caused by the frictional convergence prompted the development of the band-shaped deep precipitation clouds on the seaside region described in section 3.2. In the heavy rainfall case described in Iwanami et al. (1989), the estimated frictional convergence values ranged from  $(2.0 \text{ to } 4.0) \times 10^{-4} \text{ sec}^{-1}$  in the seaside region near Noboribetsu City. These values were determined by two methods. One used the surface winds at one site located on the coastline (B-77) and at one 5 km inland (A-57) from the coastline. The other used divergence values in the triangle area including the coastline. The estimated frictional convergence is considered to correspond to the updrafts of  $0.1 \text{ to } 0.2 \text{ ms}^{-1}$ .

The passing of a gravity wave also causes an upward motion in the atmosphere, although it does not have a direct relationship to topography. Iwanami et al. (1997a) found that the convergence values which resulted from the gravity wave with a period of 3.6 hours were  $(0.5 \text{ to } 1.8) \times 10^{-4} \text{ sec}^{-1}$  and they corresponded to the updrafts of  $0.1 \text{ to } 0.2 \text{ ms}^{-1}$ , for example, at the height of 1.0 km.

From these estimated values of updrafts caused by several possible mechanisms mentioned above, it is seen that the updrafts accompanied with synoptic scale disturbances are smaller than any other, and that the forced uplifting produced the strongest updrafts. It was therefore concluded that the updrafts over the mountainous region caused by the forced uplifting along the southeastern slope of the Orofure mountain range made the largest contribution to the convective activity and to most probably rainfall amounts in the area among these mechanisms. It was naturally considered that stronger updrafts, for example, the calculated updrafts which amounted to  $4.0 \text{ ms}^{-1}$  on the RHI cross section reported by Iwanami et al. (1997b), resulted from not only the forced uplifting and horizontal convergence by topography but also from the release of convective instability and latent heat, and further from their interactions.

## 5. Conclusions

Rainfall observations were carried out with the mobile weather radar and

special mesoscale network of raingauges, wind vanes and anemometers, and microbarometers from late August to early September in 1985 and 1986 on the southeastern slope of the Orofure mountain range in the southwestern part of Hokkaido, Japan. The rainfalls on September 3 to 4 in 1986 were associated with a depression changed from a typhoon and with northerly surface winds. The rainfall amount was distributed over wide beyond the southeastern slope of the Orofure mountain range. The stratiform radar echoes with the bright band at around 4.8 km a.s.l. extended widely over the observation area. In the first half of this rainfall, the bright band was especially remarkable and the thin distinctive layer appeared below 2.0 km a.s.l. It is considered that the thin and strong echo layer was formed by falling larger raindrops that were growing through collision and coalescence processes in a very humid lower layer. The surface winds on the southeastern slope of the mountain range were almost northerly and weak in the first half period, and it is therefore considered that the effects of topography on the precipitation clouds did not appear over this area. However, the surface winds in the region between the two ridges running southeastward changed to southerly in the second half, and the radar echoes in the lower layer were developed by the updrafts produced over the slopes blown by winds near the ground surface. Consequently the rainfall amounts around this ridge were seen to increase. It is therefore concluded that the topography produced small scale effects on the stratiform precipitation clouds passing over the observation area.

The rainfalls on September 10 to 11 in 1986 occurred under a synoptic situation where the northern part of Japan was covered with a trough and unstable atmosphere. The rainfall amount was concentrated on the southeastern slope of the Orofure mountain range, especially in the seaside region which is in contrast to the first case. The heavy rainfalls whose intensity reached  $108 \text{ mmhr}^{-1}$  at the T-31 site in the seaside region were caused by deep convective precipitation clouds that had a band-shape with about 5 km in width, 30 km in length and higher than 10 km in echo top height. It is considered that the forced uplifting of southerly flow from the Pacific Ocean near the ground surface played an important role in the generation and development of the precipitation clouds in the mountainous region. In the plain region where the geographical gradient is smaller than in the mountainous region, the precipitation clouds were considered to be maintained by the updrafts caused by the convergence over the shear line formed between northerly winds in the mountainous region and southerly winds on the seaward side. Furthermore, it is considered that the updrafts, that were caused by both the convergence over this shear line and a

frictional convergence resulting from the roughness discontinuity between land and sea, promoted the development of the band-shaped deep precipitation clouds on the seaside region.

It seems that two subjects remain to be studied in the future in order to further deeply understand the heavy rainfall mechanisms in this area. First, three-dimensional airflows in precipitation clouds are expected to be investigated through dual Doppler radar observations. At the same time, soundings by rawin sondes are needed in order to study the thermodynamics of the environment when heavy rainfalls occur and to derive the initial conditions for numerical simulations. Secondly, the microphysical processes in clouds are worthy of further detailed investigations, especially the interactions of two-layer cloud structures clarified with the radar observation by Iwanami et al. (1988). Numerical experiments by models including detailed microphysics and field observations using the dual-polarization Doppler radar or instrumented aircraft are expected.

#### Acknowledgments

The authors would like to express their sincere thanks to Dr. Y. Asuma, Meteorological Laboratory, Department of Geophysics, Faculty of Science, Hokkaido University, for his valuable discussion/advice and students in the laboratory for their support in this field work. Thanks are also due to Sapporo District Meteorological Observatory, Muroran Local Meteorological Observatory and Tomakomai Weather Station by JMA for their generous offering of useful data. This study was carried out as a link in the chain of the program of the JSPS Fellowships for Japanese Junior Scientists (K.I.). A part of the expense for this research was supported by a Grant-in-Aid for Research in Natural Disasters "Studies on the Generation Mechanisms of Local Heavy Rainfalls on the Southeastern Slope of Orofure Mountain Range in Hokkaido Island, Japan" (Project No. 61025001) and for the encouragement of Young Scientists (K.I.) (No. 02952103) of the Ministry of Education, Science, Sports and Culture of Japan.

#### References

- Bergeron, T., 1965. On the low-level redistribution of atmospheric water caused by orography. *Suppl. Proc. Int. Conf. Cloud Phys.*, Tokyo, May 1965, 96-100.
- Browning, K.A., F.F. Hill and C.W. Pardoe, 1974. Structure and mechanism of precipitation and the effect of orography in a wintertime warm sector. *Quart. J. R. Met. Soc.*, **100**, 309-330.

- Browning, K.A., C.W. Pardoe and F.F. Hill, 1975. The nature of orographic rain at winter-time cold fronts. *Quart. J. R. Met. Soc.*, **101**, 333-352.
- Harimaya, T., K. Kikuchi, T. Endoh and N. Horie, 1981. Damage caused by the heavy rainfall in the southwestern part of Hokkaido Island on August 1980. *Geophys. Bull. Hokkaido Univ.*, **40**, 113-126 (in Japanese with English abstract).
- Hill, F.F., K.A. Browning and M.J. Bader, 1981. Radar and raingauge observations of orographic rain over South Wales. *Quart. J. R. Met. Soc.*, **107**, 643-670.
- Iwanami, K., K. Kikuchi and T. Taniguchi, 1988. A possible rainfall mechanism in the Orofure mountain range Hokkaido, Japan — The rainfall enhancement by a two-layer cloud structure —. *J. Meteor. Soc. Japan*, **66**, 497-504.
- Iwanami, K., K. Kikuchi and T. Taniguchi, 1989. A case study of heavy rainfalls from the shallow orographic precipitating clouds in the Orofure mountain range, Hokkaido, Japan. *J. Fac. Sci., Hokkaido Univ., Ser. VII (Geophysics)*, **8**, 281-299.
- Iwanami, K., K. Kikuchi, H. Uyeda and T. Taniguchi, 1997a. Relationship between micro-pressure perturbation and convective activity observed in the Orofure mountain range in Hokkaido, Japan. *J. Meteor. Soc. Japan*, **75** (submitted).
- Iwanami, K., K. Kikuchi, H. Uyeda and T. Taniguchi, 1997b. Airflow circulations in the precipitation clouds observed over the Orofure mountain range in Hokkaido, Japan. *J. Meteor. Soc. Japan*, **75** (to be submitted).
- Kikuchi, K., N. Horie, T. Harimaya and T. Konno, 1988. Orographic rainfall events in the Orofure mountain range in Hokkaido, Japan. *J. Meteor. Soc. Japan*, **66**, 125-139.
- Konno, T. and K. Kikuchi, 1981. Properties of local heavy rainfall on the southeast slope of Orofure mountain range in the Iburi District, Hokkaido, Japan, (I) — Distribution patterns of rainfall amount —. *Geophys. Bull. Hokkaido Univ.*, **39**, 1-18 (in Japanese with English abstract).
- Konno, T., K. Kikuchi, K. Wakahara and K. Suzuki, 1981. Properties of local heavy rainfall on the southeast slope of Orofure mountain range in the Iburi District, Hokkaido, Japan, (II) — Simultaneous observations of the size distribution of rain drops at two raingauge stations —. *Geophys. Bull. Hokkaido Univ.*, **39**, 19-35 (in Japanese with English abstract).
- Matsumoto, S., 1974. Dynamics and structure of the mesoscale disturbances. Technical Report of JMA, **86**, 136-149 (in Japanese).
- Nakatsugawa, M., M. Takemoto and T. Yamada, 1990. Rainfall characteristics in catchment area (3) — Simulation of wind and rainfall in mountainous area —. *Mon. Rep. Civil Engineering Res. Inst.*, **447**, 20-35 (in Japanese with English abstract).
- Roeloffzen, J.C., W.D. Van Den Berg and J. Oerlemans, 1986. Frictional convergence at coastlines. *Tellus*, **38A**, 397-411.
- Sarker, R.P., 1966. A dynamical model of orographic rainfall. *Mon. Wea. Rev.*, **94**, 555-572.
- Sawyer, J.S., 1952. A study of the rainfall of two synoptic situations. *Quart. J. R. Met. Soc.*, **41**, 231-246.
- Takeda, E. and K. Kikuchi, 1978. Local heavy rainfalls in Hokkaido Island, Japn (1) — On the contribution of heavy rainfalls to the annual amount of rainfalls —. *Geophys. Bull. Hokkaido Univ.*, **37**, 19-29 (in Japanese with English abstract).
- Takeda, T., N. Moriyama and Y. Iwasaka, 1976. A case study of heavy rain in Owase area. *J. Meteor. Soc. Japan*, **54**, 32-41.
- Takeda, T. and K. Katase, 1980. Radar observation of rainfall system modified by orographic effects. *J. Meteor. Soc. Japan*, **58**, 500-516.
- Tobizuka, K. and T. Harimaya, 1989. A case study of seaside rainfall in the Iburi District, Hokkaido. *Geophys. Bull. Hokkaido Univ.*, **52**, 77-88 (in Japanese with English abstract).